Hindawi Publishing Corporation
Journal of Nanomaterials
Volume 2012, Article ID 572746, 8 pages
doi:10.1155/2012/572746

Review Article

Luminescence Properties of Si Nanocrystals Fabricated by Ion Beam Sputtering and Annealing

Sung Kim,[1] Dong Hee Shin,[1] Dong Yeol Shin,[1] Chang Oh Kim,[1] Jae Hee Park,[1] Seung Bum Yang,[1] Suk-Ho Choi,[1] Seung Jo Yoo,[2] and Jin-Gyu Kim[2]

[1] *Department of Applied Physics, College of Applied Science, Kyung Hee University, Yongin 446-701, Republic of Korea*
[2] *Division of Electron Microscopic Research, Korea Basic Science Institute, 113 Gwahangno, Yusong-gu, Daejeon 305-333, Republic of Korea*

Correspondence should be addressed to Suk-Ho Choi, sukho@khu.ac.kr

Received 1 December 2011; Revised 11 January 2012; Accepted 13 January 2012

Academic Editor: J. C. Sczancoski

During the past several decades, Si nanocrystals (NCs) have received remarkable attention in view of potential optoelectronic device applications. This paper summarizes recent progress in the study of luminescence from Si NCs, such as photoluminescence (PL), cathodoluminescence, time-solved PL, and electroluminescence. The paper is especially focused on Si NCs produced by ion beam sputtering deposition of SiO_x single layer or SiO_x/SiO_2 multilayers and subsequent annealing. The effects of stoichiometry (x) and thickness of SiO_x layers on the luminescence are analyzed in detail and discussed based on possible mechanisms.

1. Introduction

Light-emitting silicon nanocrystals (Si NCs) have attracted considerable attention since the first report on photoluminescence (PL) of porous Si in 1990 [1] was published as an effort to build Si-based photonics. Besides fundamental physics related to quantum-confinement effect (QCE) in an indirect-gap semiconductor, Si [2–5], there have been intensive studies on novel interesting phenomena such as light emission from electrically excited Si NCs or quantum dots (QDs) [6–9] and energy transfer to Er^{3+} ions [10–12], highly potential for optoelectronics applications. For realizing the device applications as well as for clarifying the origin of the observed luminescence, tight size control of Si NCs should be essential.

Si NCs can be synthesized by a number of techniques: ion implantation of Si into SiO_2 matrix [5, 13, 14], deposition of substoichiometric oxide films using chemical vapour deposition (CVD) [8, 9, 15], RF sputtering [12, 16], and reactive evaporation [17]. Most of these methods should be followed by thermal annealing procedures inducing phase separation/crystallization. The synthesized Si NCs usually have a relatively broad size distribution, which can complicate the characterization of Si NCs based on QCE and therefore is undesirable for the device applications. Ion beam sputtering deposition (IBSD) under oxygen ambient has been reported to be useful for the growth of the stoichiometric/substoichiometric oxide films [18]. This method has an advantage of providing relatively low-thermal budget, thereby producing uniform oxide films over the full depth and rendering their interface-free examination. In addition, in situ X-ray photoelectron spectroscopy (XPS) analysis during IBSD, because it enables looking into the oxidation/growth processes, is a powerful method to check the change of the chemical states on the top surface of the films.

Although Si NCs embedded in the SiO_2 exhibit efficient and tunable PL emission by changing the oxygen content (or NC size), the origin of the light emission is still under debate [19–21]. Discussions are mainly focused on whether the light emission is generated by the excitonic transitions inside Si NCs or by other defect-related centers. As reported previously, Si NCs formed in host materials such as SiO_2 have a broad distribution of size and orientation and a lot of oxygen-related defect centers exist at the interfaces of Si NCs/SiO_2 [3–5]. This explains why PL spectra of such materials have typically broad emission bands [20, 22]. The

Si=O or Si–O bonds are known to exist in the Si NCs/SiO_2 interfaces, which significantly reduce the effective optical band gap by creating localized states and pinning the band gap of Si NCs, resulting in the PL peak shift smaller than expected from QCE [23–25].

Even though there have been some technological advances in producing Si-NC-based light emitting diodes (LEDs) in the form of a metal oxide semiconductor (MOS LEDs) [6, 25, 27], no breakthrough for the efficient devices has been reported yet. One of the main obstacles in the production of efficient MOS LEDs is the problem of carrier injection into the insulating oxide matrix. Several models have been proposed for explaining the carrier injection processes, which are still in controversy. In addition to studies on electroluminescence (EL) as well as on PL, those on their correlations are especially needed for understanding the mechanisms of charge injection and light generation, thereby clarifying the operation principles of MOS LEDs.

In this paper, we review luminescence properties of Si NCs studied by continuous-wave/time-resolved PL, cathodoluminescence (CL), and EL spectroscopies and discuss their size-dependent correlations based on possible light-emitting mechanisms.

2. Experimental Details

SiO_x single-layer (SL) films of $2 \sim 200$ nm and SiO_x/SiO_2 multilayers (MLs) with 50 periods of 2 nm thin layers were grown on n-type (100) Si wafers at room temperature (RT) using an Ar^+ beam with an ion energy of 750 eV and a Si target under oxygen atmosphere in a reactive IBSD system with a Kaufman-type DC ion gun. The relative film thickness was controlled from the growth rate calibrated by transmission electron microscopy (TEM) measurements of thin films grown within a given time. The deposition chamber was evacuated to a pressure of 5.0×10^{-9} torr before introducing argon gas into the system. Details of the system are described elsewhere [18]. The stoichiometry of the SiO_x films could be analyzed and controlled with in situ XPS using Al $k\alpha$ line of 1486.6 eV. A stoichiometric SiO_2 thin film was used as a reference for the determination of the relative sensitivity factors of Si 2p and O 1s peaks. The B doping of the SiO_x layers was achieved by cosputtering using a combination target where a small boron chip was fixed on a p-type Si wafer. The doping concentration was controlled by varying the size of the boron chip. The doping level of the SiO_x layers was estimated by secondary ion mass spectroscopy (Cameca, model IMS-7f) using an oxygen-ion beam of 5 keV. The quantification of the B-doped SiO_x layers was performed using a B-implanted certified reference material. After deposition, the samples were annealed at 1100°C in an ultrapure nitrogen ambient by using a horizontal furnace to form Si NCs in the layers. In order to passivate Si dangling bonds, some of the samples were hydrogenated by heating the samples at 650°C for 60 min under H_2 flow.

PL spectra were measured at RT using the 325 nm line of a HeCd laser as the excitation source. Emitted light was collected by a lens and analysed using a grating monochromator and a GaAs photomultiplier (PM) tube. Standard lock-in detection techniques were used to maximize the signal-to-noise ratio. The laser beam diameter was about 0.3 mm and the power was about 3 mW. The excitation for time-resolved PL was done by a pulsed Nd:YAG laser (wavelength: 355 nm, pulse energy density: 0.6 mJ/cm^2, repetition frequency: 20 Hz, and pulse duration: 20 ps). The emitted light was analyzed by using a monochromator equipped with a gated intensified charge-coupled device (CCD) (detection energy: $1.38 \sim 9.92$ eV and response time: 40 ps, PI-Max, Princeton Instrument) triggered by exciting laser pulse. CL spectra were measured in the range of electron beam energies of 1 to 20 kV by using a JEOL 6330F field emission scanning electron microscope equipped with an Oxford Instrument Mono CL2. The CL spectra were dispersed by a 1200 lines/mm grating blazed at 500 nm and detected using a Hamamatsu R943-02 peltier-cooled PM tube. The current-voltage (I-V) curves of the LED devices were measured using Keithley 237 high-voltage source meter. For forward-bias conditions, positive voltages were applied to the Al contacts on the poly-Si layers of LED devices. The RT EL measurements were performed under forward bias by using DM 500 grating monochromator equipped with a Si CCD for light detection.

3. Results and Discussion

3.1. Continuous-Wave Photoluminescence. Figure 1(a) shows thickness dependence of the PL spectra for Si-NC SLs with $x = 1.4$. The major PL band in the range of 765 to 850 nm has been widely observed and attributed to the radiative recombination of quantum-confined electrons and holes in Si NCs [14, 21]. The PL spectra are redshifted monotonically with increasing the SiO_x thickness (d) due to the size increase of Si NCs in thicker samples. Previously, it has been similarly reported that larger NCs grow in thicker SiO_x [28]. Figure 1(b) summarizes the PL peak shift as a function of d at each x. For $x \leq 1.2$, the PL peaks show a rather confusing behavior, that is, weak blueshifts with increasing d. For $x \geq 1.4$, the PL peaks show monotonic redshifts as d increases, consistent with QCE.

A few nm thick natural SiO_2 is usually formed on the surface of the SiO_x layer after deposition, thereby reducing the real thickness of SiO_x. During annealing, the NC size could be strongly influenced by the mixing of SiO_x with SiO_2, which exists at the bottom interface of the SiO_x layer/Si wafer as well as on the top surface of SiO_x, resulting in an increase of x value [19]. This is reasonable because the mixing during annealing can occur within a diffusion distance of Si in SiO_x matrix that was reported to be as long as about 3 nm [29]. The SiO_2 layer would make a stronger effect on the stoichiometry of thinner SiO_x layer. These considerations can explain why the PL peaks are located at smaller wavelengths in the samples with thinner SiO_x layers, as shown in Figure 1(b).

It is possible to independently control NC size/density by employing a technique of ML growth for Si NCs [21, 28, 30]. The layer thickness/excess Si content of Si-rich oxide (SiO_x) in the ML structures of SiO_x/SiO_2 determines the NC size/density, respectively, after high-temperature

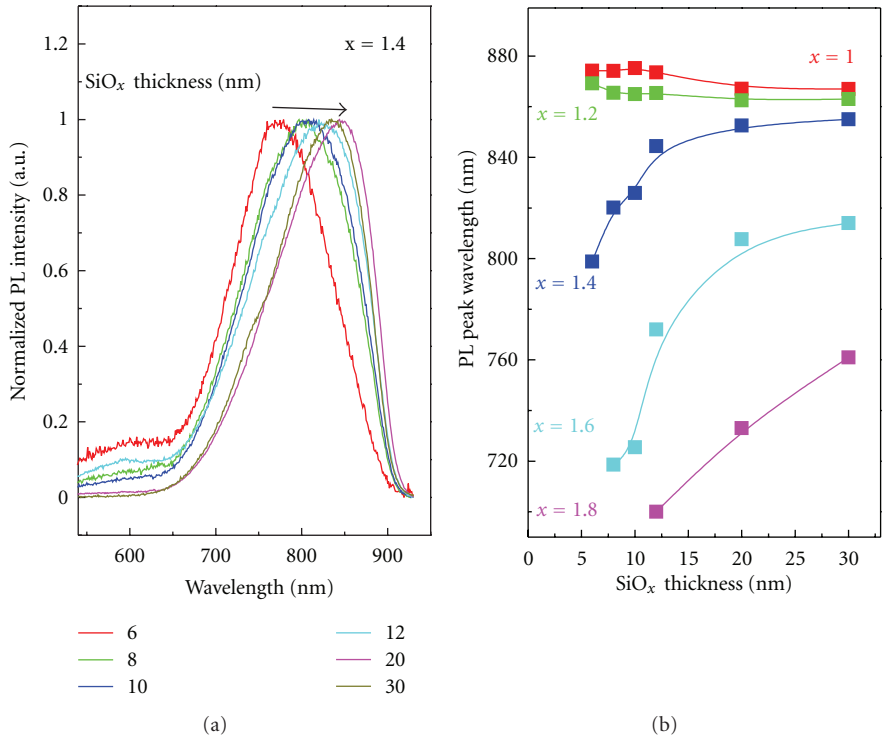

Figure 1: (a) SiO_x-layer-thickness-dependent PL spectra for single-layer (SL) Si NCs with $x = 1.4$. (b) PL peak shifts as functions of SiO_x-layer thickness at each x [21, 26].

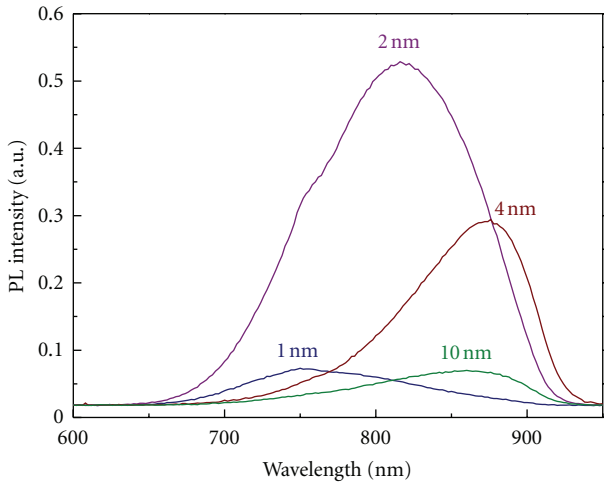

Figure 2: PL spectra of SiO_x/SiO_2 MLs after annealing at 1100°C for various thicknesses of the SiO_x layer [21].

annealing. This approach can make it possible to engineer the energy of the band gap of Si NCs by optimizing the thickness/composition in the ML structures of Si NC/SiO_2. Figure 2 shows RT PL spectra of SiO_x/SiO_2 MLs after annealing for various thicknesses of the SiO_x layer. The PL spectra are blueshifted with decreasing d, with their maximum intensity at $d = 2$ nm.

Figure 3(a) shows a cross-sectional high-resolution TEM (HRTEM) image of 50-period 2 nm $SiO_{1.0}$/2 nm SiO_2 MLs after annealing at 1100°C, in which the ML structure and the phase separation are clearly observed. Using full-size HRTEM images, the average size and density of the Si NCs are estimated to be $\sim 3.8 \pm 0.8$ nm and 3.5×10^{12} cm^{-2}, respectively. Figure 3(b) compares full widths at half maximum (FWHMs) of PL spectra between ML and SL samples ($x = 1.0$) with the same total thickness of 200 nm. The PL spectra of both samples are almost identically peaked at around 860 nm (1.44 eV), in agreement with the estimated recombination energy for quantum-confined excitons in a ~3.5 nm diameter Si NCs [28]. The PL FWHM (70 nm) of ML sample is much smaller than that of SL sample (103 nm), indicating more-uniform-size distribution of Si NCs in ML samples, still valid for other x values, as shown in Figure 3(c). Figure 3(c) also shows the size-dependent PL peak shifts consistent with QCE for both samples.

3.2. Cathodoluminescence. It is hard to interpret the CL spectra of Si NCs based on the QCE effect because the CL emissions are sometimes mixed with those from the interface or surface defect states in the similar energy ranges [31, 32]. Recently, CL spectra of Si nanoparticles below 3 nm in porous Si have given an evidence of the CL light emission in the UV range from ultrasmall Si NCs [32]. In our previous work, a CL emission at 2.16 eV (574 nm) has been ascribed to 3.5 nm Si NCs formed in Al_2O_3 by ion implantation [33]. Figure 4(a) shows CL spectra of Si-NC MLs at each x after hydrogenation, which were measured by using an electron beam energy of 15 keV at 77 K. Two major CL bands are

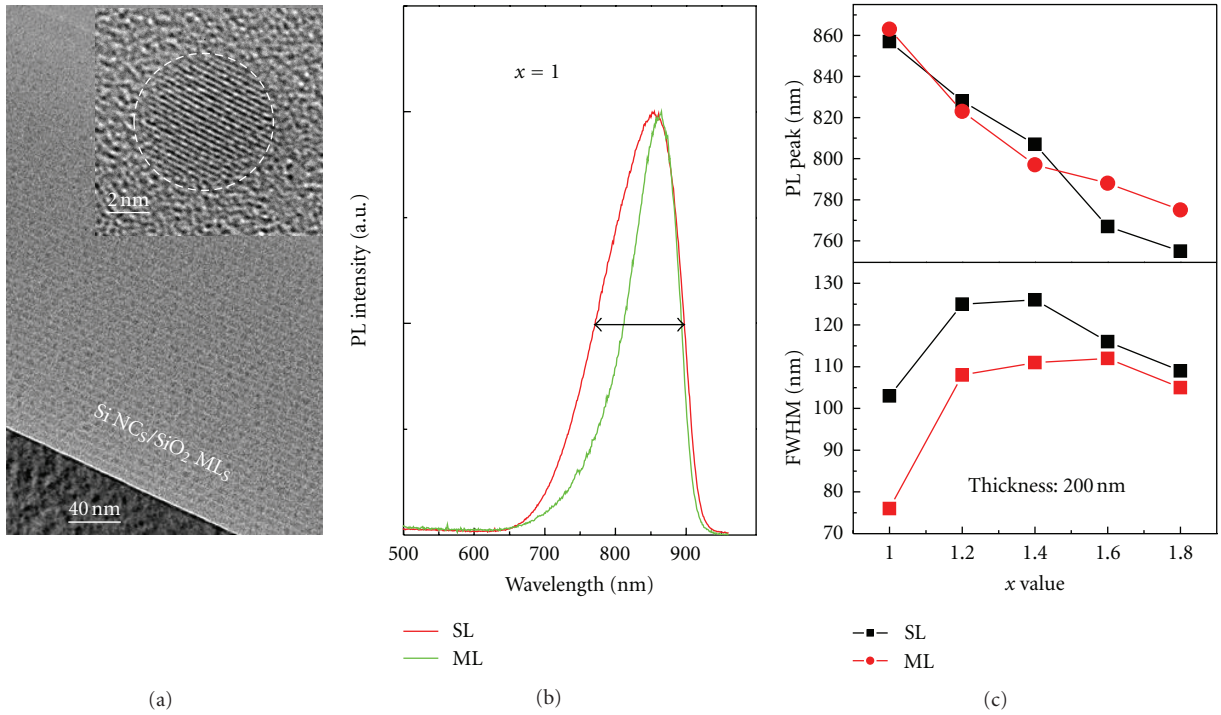

FIGURE 3: (a) Cross-sectional HRTEM image of 50-period 2 nm $SiO_{1.0}$/2 nm SiO_2 MLs after annealing at 1100°C. (b) FWHMs of normalized PL spectra for ML and SL samples with the same total thickness of 200 nm. (c) Size-dependent PL peak energy and FWHMs of ML and SL samples.

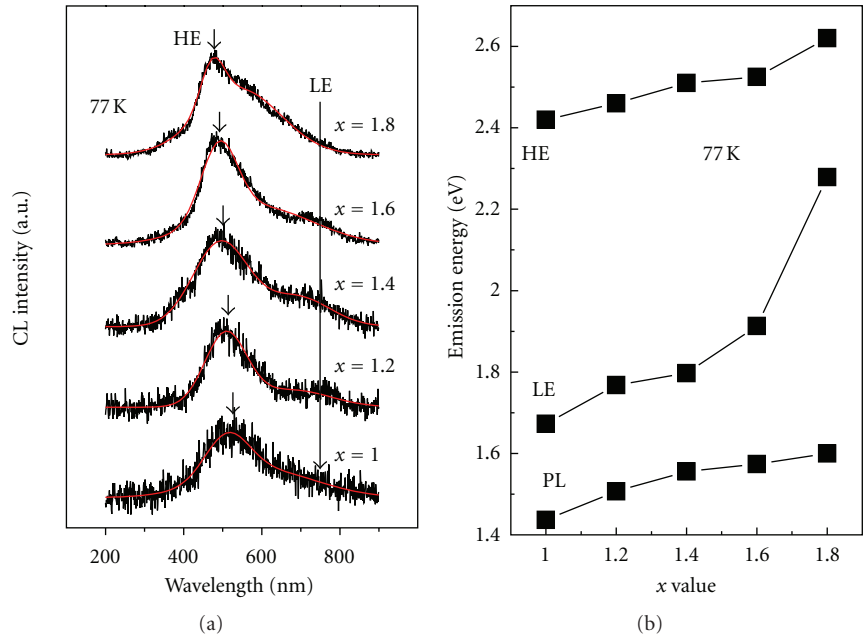

FIGURE 4: (a) CL spectra of the ML Si NCs at each x after hydrogenation. (b) Energy shifts of the deconvoluted CL (HE and LE) and PL bands as functions of x [22].

observed at ~1.66 eV (750 nm) and ~2.18 eV (570 nm) at $x = 1.0$, which are named low-energy (LE) and high-energy (HE) bands, respectively. The CL spectra were deconvoluted into two Gaussian bands in order to find peak positions of the HE and LE bands accurately. Figure 4(b) compares energy shifts of the deconvoluted CL bands with those of PL band as functions of x. The HE (LE) CL band is blueshifted from 2.18 (1.66) to 2.64 (2.16) eV, respectively, as x increases from 1.0 to 1.8. The total energy shift of the CL bands is more than two times as large as that of the PL band.

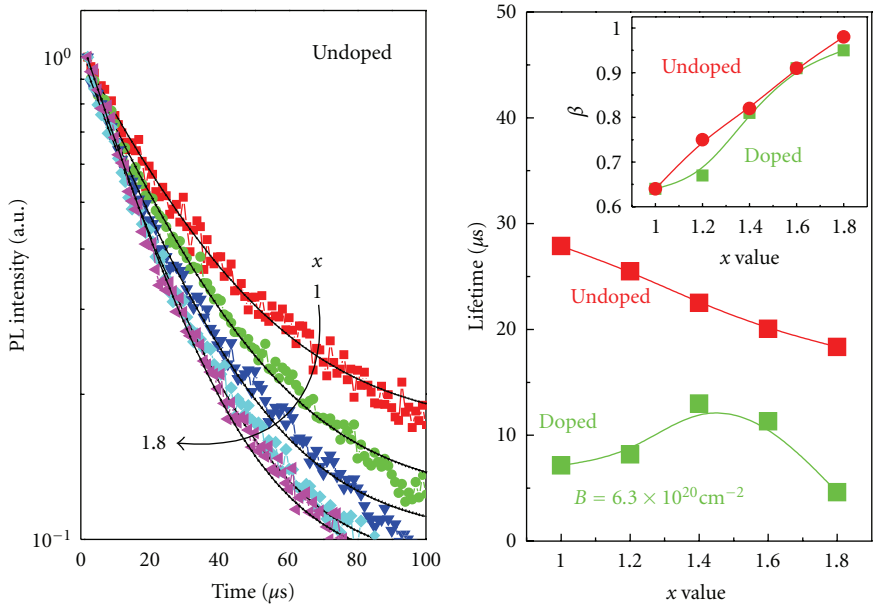

FIGURE 5: (a) PL decay curves of undoped ML Si NCs at 300 K for various x values. (b) Lifetimes as functions of x for undoped and B-doped Si NCs. The inset shows β values as functions of x for both samples.

The CL spectra exhibit very different behaviors at 300 K [22]. A new strong CL band appears at about 2.70 eV (460 nm) without almost any energy shift with x. The 2.70 eV peak has been attributed to amorphous SiO_2 defects in porous Si [31] or localized defects at the Si/SiO_2 interface [31, 32]. The HE band still remains at around 2.39 eV (520 nm) even in the 300 K spectra, but no peak shift with x is seen due to the dominant effect of the defect CL band. At 77 K, the defect CL band disappears, as shown in Figure 4(a), consistent with the observation that the defect-related CL band is reduced at lower temperature [31]. These results suggest that the CL band originating from Si NCs can be well analyzed at low temperature and reflect the size dependence of the peak shifts better than the PL band.

3.3. Time-Resolved Photoluminescence. The carrier relaxation and dynamics by state filling and migration [26, 34–36] are interesting phenomena involved in the light-emission processes of semiconductor nanostructures. The state-filling effect of Si NCs has been studied for discussing the parabolic confinement of Si NCs and the energy splitting between the energy levels [36]. Migration of the excitons between neighboring Si NCs has been shown to influence their optical properties [35, 36]. The migration process involves thermalization of the excitons, meaning the migration of excitons into the energetically most favorable low-energy states.

Figure 5(a) shows PL decay curves of undoped Si-NC MLs at 300 K. PL decay traces were measured for x values in the range of 1.0 to 1.8 and well fitted to a stretched exponential function, $I(t) = I_0 \exp[-(t/\tau_{PL})^{\beta}]$ [4, 18–20], where I_0 is the PL intensity at $t = 0$, τ_{PL} the effective PL lifetime, and β the dispersion factor having a value between 0 and 1. τ_{PL} for each x was obtained by fitting the decay traces taken at the peak wavelength in the PL spectra. The fitted results are drawn by solid lines in Figure 5(a). Figure 5(b) summarizes the variations of the lifetimes as functions of x for undoped and B-doped Si NCs. The lifetime of undoped Si NCs increases monotonically with decreasing x. The lifetime of B-doped Si NCs increases from 4.6 to 13.0 μs as x varies from 1.8 to 1.4, but by further decrease of x, it decreases.

As previously reported for undoped Si NCs by us [26, 34], the PL lifetime as well as the PL radiative lifetime showed monotonically increasing behaviors with increasing the size of NCs (decreasing x), possibly due to the reduction in the relative portion of the interface states between SiO_2 and NCs in the samples containing larger Si NCs [22]. In contrast, in doped Si NCs, the PL lifetime decreases with decreasing x (increasing the NC size) below 1.4, as shown in Figure 5(b), resulting from the increase of optically less active NCs by the increase of NCs containing more dopants at larger NC sizes. Optically less active NCs would affect the lifetime of neighboring NCs by the effect of coupling between the closely packed NCs [26], resulting in a reduction of the lifetime in the latter.

The inset of Figure 5(b) compares x-dependent β values for undoped and B-doped NCs, both of which show similar monotonic increasing behaviors with increasing x. The stretched line shape of the PL decay originates from a system of interacting Si NCs in which migration of excitons occurs [26, 36]. The dispersion factor β indicates a measure of the migration process [37]. For totally isolated NCs, β approaches 1, indicating a single exponential time decay of their PL signal. At smaller x (larger NCs), some interference is expected between adjacent NCs by tunneling of excitons

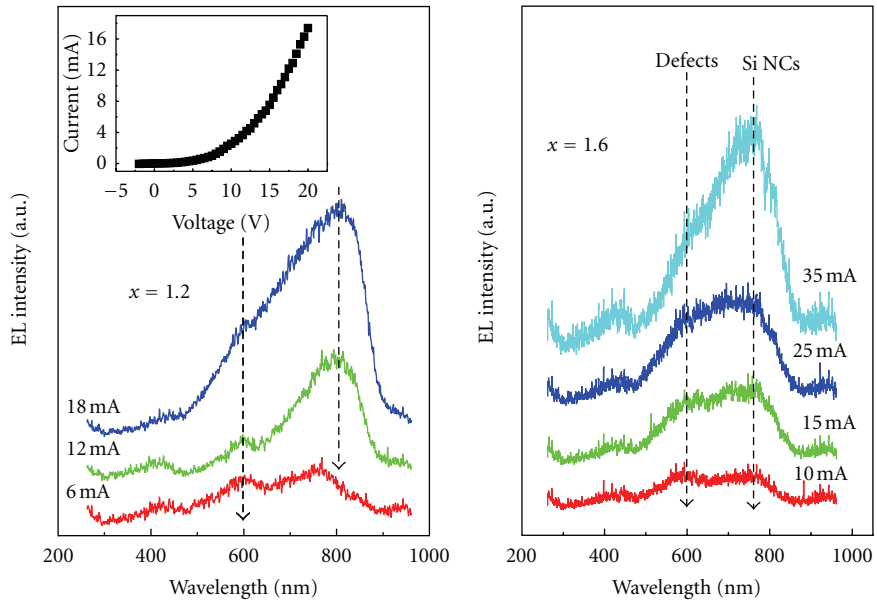

Figure 6: (a) EL spectra of a LED device containing Si NC MLs with $x = 1.2$ for various injection currents. The inset shows the I-V curve. (b) EL spectra of a LED device with $x = 1.6$ for various injection currents.

through the thin oxide between NCs, affecting the degree of exciton localization. Smaller NCs are more distant, resulting in stronger localization of excitons, thereby increasing β with increasing x, as shown in the inset of Figure 5(b). These results also suggest that doping would not affect the size-dependent behaviors of the exciton migration.

3.4. Electroluminescence. For fabricating MOS-LEDs [37, 38], 200 nm thick Si-NC MLs were formed on p^+-type Si wafers as a dielectric layer. A highly n^+-type 50 nm thick poly-Si layer was deposited on top of the Si-NC MLs by low-pressure CVD. The poly-Si layer would improve the efficiency of electron injection into Si NCs in the oxide layer. Then, a circular area of 0.3 mm in diameter was defined for the active area of the device by using standard photolithography. Finally, Al-based contacts defined as circular rings were fabricated on the polysilicon film and the Si substrate. The wide central area of the device is metal free to allow the exit of the light.

Figure 6(a) shows EL spectra of a typical LED device containing Si-NC MLs with $x = 1.2$ for various injection currents. The EL emission band originating from Si NCs is observed at around 800 nm, which is smaller than the PL peak wavelength, as shown in Figure 3(c). The EL peak wavelength shows no clear injection current dependence. Another EL band appears at around 600 nm, which is thought to originate from defect states at the interfaces of Si NCs/SiO_2 or SiO_2/Si substrate [6, 9]. The LED devices were also fabricated for various sizes of Si NCs by varying x value. Figure 6(b) shows a typical blueshift of the EL peak at $x = 1.6$ due to the size reduction of Si NCs. In contrast, the defect-related EL peak is almost fixed at around 600 nm, irrespective of the size variation of Si NCs. All LED devices showed good rectifying behaviors, as shown in the inset of Figure 6(a).

4. Conclusion

SiO_x SL films and SiO_x/SiO_2 MLs were grown on n-type Si wafers by IBSD. The B doping of the SiO_x layers was achieved by cosputtering using a combination target of a p-type Si wafer with a small boron chip on its center. The samples were annealed at 1100°C under nitrogen ambient to form Si NCs in the SiO_x layers. The size of Si NCs and corresponding PL peak energy were strongly dependent on the thickness of the SiO_x layer as well as its stoichiometry. The MLs shown to be more uniform in size than the SLs were turned out to be more useful for the characterization of Si NCs based on QCE and their device applications. The CL band originating from Si NCs could be well analyzed at low temperature and reflected the size dependence of the peak shifts better than the PL band. B doping of Si NCs resulted in the reduction of PL lifetime for larger NCs, possibly due to the increase of optically less active NCs. The decay traces of time-resolved PL spectra reflected the size dependence of the exciton migration, which was not influenced by B doping of Si NCs. The properties of EL from LEDs containing Si NC MLs were shown to be consistent with QCE by varying their size.

Acknowledgments

This work was supported by a National Research Foundation of Korea (NRF) grant funded by the Korean government (Ministry of Education, Science and Technology (MEST)), (no. 2010-00771) and a grant from the Kyung Hee University in 2010 (KHU-20100171) and was performed using the high-voltage electron microscope (JEM-ARM1300S, Jeol, Japan) installed at Korea Basic Science Institute.

References

[1] L. T. Canham, "Silicon quantum wire array fabrication by electrochemical and chemical dissolution of wafers," *Applied Physics Letters*, vol. 57, no. 10, pp. 1046–1048, 1990.

[2] D. Kovalev, H. Heckler, M. Ben-Chorin, G. Polisski, M. Schwartzkopff, and F. Koch, "Breakdown of the k-conservation rule in Si nanocrystals," *Physical Review Letters*, vol. 81, no. 13, pp. 2803–2806, 1998.

[3] S. Godefroo, M. Hayne, M. Jivanescu et al., "Classification and control of the origin of photoluminescence from Si nanocrystals," *Nature Nanotechnology*, vol. 3, no. 3, pp. 174–178, 2008.

[4] M. L. Brongersma, P. G. Kik, A. Polman, K. S. Min, and H. A. Atwater, "Size-dependent electron-hole exchange interaction in Si nanocrystals," *Applied Physics Letters*, vol. 76, no. 3, pp. 351–353, 2000.

[5] L. Pavesi, L. Dal Negro, C. Mazzoleni, G. Franzò, and F. Priolo, "Optical gain in silicon nanocrystals," *Nature*, vol. 408, no. 6811, pp. 440–444, 2000.

[6] M. Wang, X. Huang, J. Xu, W. Li, Z. Liu, and K. Chen, "Observation of the size-dependent blueshifted electroluminescence from nanocrystalline Si fabricated by KrF excimer laser annealing of hydrogenated amorphous silicon/amorphous-SiN_X:H superlattices," *Applied Physics Letters*, vol. 72, no. 6, pp. 722–724, 1998.

[7] K.-Y. Cheng, R. Anthony, U. R. Kortshagen, and R. J. Holmes, "High-efficiency silicon nanocrystal light-emitting devices," *Nano Letters*, vol. 11, no. 5, pp. 1952–1956, 2011.

[8] A. Anopchenko, A. Marconi, M. Wang, G. Pucker, P. Bellutti, and L. Pavesi, "Graded-size Si quantum dot ensembles for efficient light-emitting diodes," *Applied Physics Letters*, vol. 99, no. 18, Article ID 181108, 2011.

[9] Z. Liu, J. Huang, P. C. Joshi et al., "Polarity-controlled visible/infrared electroluminescence in Si-nanocrystal/Si light-emitting devices," *Applied Physics Letters*, vol. 97, no. 7, Article ID 071112, 2010.

[10] P. G. Kik and A. Polman, "Gain limiting processes in Er-doped Si nanocrystal waveguides in SiO_2," *Journal of Applied Physics*, vol. 91, no. 1, pp. 534–536, 2002.

[11] P. G. Kik, M. L. Brongersma, and A. Polman, "Strong exciton-erbium coupling in Si nanocrystal-doped SiO_2," *Applied Physics Letters*, vol. 76, no. 17, pp. 2325–2327, 2000.

[12] I. Izeddin, D. Timmerman, T. Gregorkiewicz et al., "Energy transfer in Er-doped SiO_2 sensitized with Si nanocrystals," *Physical Review B*, vol. 78, no. 3, Article ID 035327, 2008.

[13] M. Perálvarez, J. Barreto, J. Carreras et al., "Si-nanocrystal-based LEDs fabricated by ion implantation and plasma-enhanced chemical vapour deposition," *Nanotechnology*, vol. 20, no. 40, Article ID 405201, 2009.

[14] M. L. Brongersma, A. Polman, K. S. Min, E. Boer, T. Tambo, and H. A. Atwater, "Tuning the emission wavelength of Si nanocrystals in SiO_2 by oxidation," *Applied Physics Letters*, vol. 72, no. 20, pp. 2577–2579, 1998.

[15] G. R. Lin, C. J. Lin, and C. T. Lin, "Low-plasma and high-temperature PECVD grown silicon-rich SiO_x film with enhanced carrier tunneling and light emission," *Nanotechnology*, vol. 18, no. 39, Article ID 395202, 2007.

[16] H. Seifarth, R. Grötzschel, A. Markwitz, W. Matz, P. Nitzsche, and L. Rebohle, "Preparation of SiO_2 films with embedded Si nanocrystals by reactive r.f. magnetron sputtering," *Thin Solid Films*, vol. 330, no. 2, pp. 202–205, 1998.

[17] S. Zhang, W. Zhang, and J. Yuan, "The preparation of photoluminescent Si nanocrystal-SiO_x films by reactive evaporation," *Thin Solid Films*, vol. 326, no. 1-2, pp. 92–98, 1998.

[18] K. J. Kim, D. W. Moon, S. H. Hong et al., "In situ characterization of stoichiometry for the buried SiO_x layers in SiO_x/SiO_2 superlattices and the effect on the photoluminescence property," *Thin Solid Films*, vol. 478, no. 1-2, pp. 21–24, 2005.

[19] M. C. Kim, Y. M. Park, S. H. Choi, and K. J. Kim, "Photoluminescence characterization of dependence of Si-nanocrystals formation in Si-rich SiO_x on thickness, oxygen content, and the existence of a SiO_2 cap layer," *Journal of the Korean Physical Society*, vol. 50, no. 6, pp. 1760–1763, 2007.

[20] S. Kim, M. C. Kim, S. H. Choi, K. J. Kim, H. N. Hwang, and C. C. Hwang, "Size dependence of Si 2*p* core-level shift at Si nanocrystal/ SiO_2 interfaces," *Applied Physics Letters*, vol. 91, no. 10, Article ID 103113, 2007.

[21] S. H. Hong, S. Kim, S. H. Choi et al., "Optical characterization of Si nanocrystals in Si-rich SiO_x and SiO_x/SiO_2 multilayers grown by ion beam sputtering," *Journal of the Korean Physical Society*, vol. 45, no. 1, pp. 116–119, 2004.

[22] S. Kim, Y. M. Park, S. H. Choi, and K. J. Kim, "Origin of cathodoluminescence from Si nanocrystal/SiO_2 multilayers," *Journal of Applied Physics*, vol. 101, no. 3, Article ID 034306, 2007.

[23] X. X. Wang, J. G. Zhang, L. Ding et al., "Origin and evolution of photoluminescence from Si nanocrystals embedded in a SiO_2 matrix," *Physical Review B*, vol. 72, no. 19, Article ID 195313, pp. 1–6, 2005.

[24] M. V. Wolkin, J. Jorne, P. M. Fauchet, G. Allan, and C. Delerue, "Electronic states and luminescence in porous silicon quantum dots: the role of oxygen," *Physical Review Letters*, vol. 82, no. 1, pp. 197–200, 1999.

[25] A. Irrera, F. Iacona, I. Crupi et al., "Electroluminescence and transport properties in amorphous silicon nanostructures," *Nanotechnology*, vol. 17, no. 5, pp. 1428–1436, 2006.

[26] S. Kim and S. H. Choi, "Size-dependent correlation of the photoluminescence lifetime with Si suboxide states at Si nanocrystal/SiO_2 interfaces," *Journal of the Korean Physical Society*, vol. 52, no. 2, pp. 462–465, 2008.

[27] Y. Liu, T. P. Chen, L. Ding et al., "Influence of charge trapping on electroluminescence from Si-nanocrystal light emitting structure," *Journal of Applied Physics*, vol. 101, no. 10, Article ID 104306, 2007.

[28] M. Zacharias, J. Heitmann, R. Scholz, U. Kahler, M. Schmidt, and J. Bläsing, "Size-controlled highly luminescent silicon nanocrystals: a SiO/SiO_2 superlattice approach," *Applied Physics Letters*, vol. 80, no. 4, pp. 661–663, 2002.

[29] L. A. Nesbit, "Annealing characteristics of Si-rich SiO_2 films," *Applied Physics Letters*, vol. 46, no. 1, pp. 38–40, 1985.

[30] V. Osinniy, S. Lysgaard, V. Kolkovsky, V. Pankratov, and A. Nylandsted Larsen, "Vertical charge-carrier transport in Si nanocrystal/SiO_2 multilayer structures," *Nanotechnology*, vol. 20, no. 19, Article ID 195201, 2009.

[31] L. H. Abuhassan, M. R. Khanlary, P. Townsend, and M. H. Nayfeh, "Cathodoluminescence of small silicon nanoparticles under electron-beam excitation," *Journal of Applied Physics*, vol. 97, no. 10, Article ID 104314, pp. 1–5, 2005.

[32] G. Belomoin, J. Therrien, A. Smith et al., "Observation of a magic discrete family of ultrabright Si nanoparticles," *Applied Physics Letters*, vol. 80, no. 5, pp. 841–843, 2002.

[33] C. J. Park, Y. H. Kwon, Y. H. Lee et al., "Origin of luminescence from Si^--implanted (1102) Al_2O_3," *Applied Physics Letters*, vol. 84, no. 14, pp. 2667–2669, 2004.

[34] S. Kim, Y. Min Park, S. H. Choi, K. Joong Kim, and D. Hoon Choi, "Temperature-dependent carrier recombination processes in nanocrystalline Si/SiO_2 multilayers studied by continuous-wave and time-resolved photoluminescence," *Journal of Physics D*, vol. 40, no. 5, article 005, pp. 1339–1342, 2007.

[35] S. Kim, Y. M. Park, S. H. Choi, and K. J. Kim, "Time-integrated and time-resolved photoluminescence properties of Si nanocrystal/SiO_2 multilayers grown by ion-beam sputtering," *Journal of the Korean Physical Society*, vol. 50, no. 3, pp. 567–570, 2007.

[36] L. Van Dao, X. Wen, M. T. T. Do et al., "Time-resolved and time-integrated photoluminescence analysis of state filling and quantum confinement of silicon quantum dots," *Journal of Applied Physics*, vol. 97, no. 1, Article ID 013501, 2005.

[37] J. Heitmann, F. Müller, L. Yi, M. Zacharias, D. Kovalev, and F. Eichhorn, "Excitons in Si nanocrystals: confinement and migration effects," *Physical Review B*, vol. 69, no. 19, Article ID 195309, 2004.

[38] A. Irrera, F. Iacona, I. Crupi et al., "Electroluminescence and transport properties in amorphous silicon nanostructures," *Nanotechnology*, vol. 17, no. 5, pp. 1428–1436, 2006.